

# Blockage Avoidance in Relay Paths for Roadside mmWave Backhaul Networks

Yuchen Liu, Qiang Hu, and Douglas M. Blough

School of Electrical and Computer Engineering, Georgia Institute of Technology, Atlanta, GA, 30332

**Abstract**—With the increasing use of bandwidth-hungry applications on mobile devices, mmWave communication is considered a key enabling technology for 5G cellular networks. One very promising use of mmWave communication is in wireless backhaul for 5G. In this paper, we consider wireless backhaul links deployed along the side of a road, which will be a common scenario both in urban environments and on highways. We investigate blockage robustness within an interference-free topology previously proposed for roadside wireless backhaul. Reconfiguration algorithms are provided both for the case where rescheduling is possible after reconfiguration and for the case that the original transmission schedule must be maintained. We prove that our reconfiguration algorithms are guaranteed to maintain connectivity under several obstacle scenarios. We also evaluate the algorithms’ performance with varying numbers of randomly-placed obstacles through simulation. Results show that our algorithms not only achieve high throughputs close to the no-blockage case, but also provide high blockage tolerance rates for the common case of a few obstacles along a several hundred meter section of a road.

## I. INTRODUCTION

In recent years, millimeter wave (mmWave) communication has been heavily researched for its potential to provide ultra high speed wireless communication with individual link rates over tens of gigabits per second [1]. Because of this potential, mmWave is considered as a key enabling technology for applications such as real-time HD-video streaming and virtual reality in 5G cellular networks as well as WPANs and WLANs.

However, there are a number of problems with mmWave communication that must be overcome for its full potential to be realized. The first problem is higher path loss compared to lower-frequency communication. To address this, the use of high-gain directional antennas can help compensate for the poor mmWave signal propagation characteristics and also reduce the interference footprint of mmWave communications. Another significant challenge for mmWave communication loss is the blockage effect when an obstacle blocks the line-of-sight (LOS) path between transmitter and receiver. Because electromagnetic waves do not diffract well around obstacles with larger sizes than their wavelength [2], mmWave links are easily blocked by obstacles such as buildings, vehicles, or even humans, and signal strength is degraded by about 30dB for non-LOS paths [3].

One promising use case for mmWave communication is wireless backhaul [4], [5], where a large number of small-cell base stations (BSs) without any wired

connections form a mesh network to carry traffic to/from designated nodes that serve as gateways to the wired infrastructure. Due to the high traffic demands in backhaul scenarios, mmWave is very well suited for the backhaul mesh links. To achieve sufficiently-high data rates for backhaul and to avoid large permanent obstacles such as tall buildings in urban environments, a number of papers have suggested the use of mmWave relay nodes to connect BS pairs in the mesh backhaul [4], [5], [12].

For blockage handling problems in mmWave wireless networks, most previous works focus on indoor settings [6], [7], which utilize reflections to provide some blockage resilience, but the transmissions suffer from severe signal attenuation due to the absorption of reflecting surface at mmWave frequencies. Other research uses relays to maintain connectivity [8], [9], but just considers multi-AP diversity and a small number of relays, which are not sufficient to maintain high data rates in outdoor environments. To our knowledge, there are only a few works that have considered multi-hop relay paths for blockage avoidance in outdoor environments [10], [11]. Particularly, [11] finds multi-hop relay paths within a single mmWave cell, but it is primarily concerned with finding a relay path with the highest probability of reaching the BS. In contrast, our work considers the maintenance of relay paths with very high rates in the presence of temporary blockages.

In this paper, we consider mmWave relays deployed along roadsides in urban environments, such as was proposed in [4], [12]. In [12], it was shown that by mounting nodes on regularly-spaced lampposts according to a *triangular-wave topology*, interference among the links on a path of mmWave nodes (referred to as self interference) can be eliminated, thereby maximizing end-to-end throughput. However, depending on lamppost height, these deployments could be susceptible to obstacles in the form of large trucks or other objects that could block some of the LOS paths between consecutive nodes. Fig. 1 shows such a situation where a truck’s height is greater than the height of a lamppost. In this paper, we consider how to handle blockages in this roadside-deployment scenario. Our approach is to reconfigure mmWave paths by dynamically steering mmWave beams to avoid obstacles. We present algorithms for reconfiguring mmWave paths that guarantee blockage tolerance with reasonable assumptions about obstacle size and frequency. Through simulation, we also evaluate the performance of the reconfigured paths constructed

by our algorithms under random obstacle scenarios. The results show that our algorithms provide robust blockage tolerance and achieve throughputs close to the no-blockage case.



Fig. 1. A parked truck next to a lamppost in an urban environment.

## II. SYSTEM OVERVIEW

In this section, we introduce our network model, including the model for relay-assisted mmWave mesh backhaul links, the channel and antenna models, and a novel blockage model used in our proposed schemes.

### A. Relay-Assisted mmWave Mesh Links

With the advent of 5G, deploying mmWave small cell BSs along roadsides will be necessary to provide high data rate service to vehicles and their passengers. As discussed in [4], [12], these deployments will likely require the use of mmWave relays along the roadsides in between the small cell BSs. A traditional “straight-line” topology, which mounts these relays on the tops of lampposts in a straight line, leads to poor system throughput due to severe self interference, and very limited ability to handle obstacles that block any of the links. Therefore, we adopt the “triangular-wave” topology for relay-assisted backhaul, which is depicted in the blue links of Fig. 2. In this topology, BSs and relays are deployed on equally-spaced lampposts on both sides of a road. With equally-spaced lampposts, the angle  $\theta$  between the center of a mmWave beam and the side of the road and the distance  $d_0$  between the locations of consecutive nodes projected onto the same side of the road are the same everywhere along the topology.

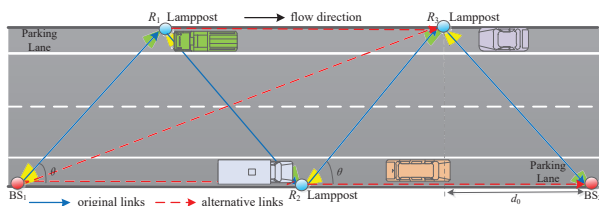


Fig. 2. Topology model of relay-assisted mmWave backhaul.

One important feature of the triangular-wave topology is that with a large enough  $\theta$  relative to the beamwidth of the mmWave directional antennas, self interference along the path is eliminated. In our previous work (Theorem 1 in [12]), we proved that the following condition is necessary and sufficient to eliminate self-interference in the triangular-wave topology:

$$\theta - \arctan\left(\frac{\tan \phi}{3}\right) > \frac{\phi}{2} \quad (1)$$

where  $\phi$  is the beamwidth of the flat-top directional antennas used along the path. Because mmWave allows a high antenna density, narrow beamwidth directional antennas can be achieved through beamforming. As an example, with a beamwidth of  $15^\circ$ , Eq. 1 yields an angle  $\theta$  of only around  $12^\circ$ . With such a small angle, the link length is increased by only a small amount compared to the straight-line topology but links become interference free, increasing the end-to-end throughput substantially. In this paper, we investigate another potential advantage of the triangular-wave topology, namely the ability to reconfigure it to avoid obstacles that might occur along the roadway. In what follows, we refer to this interference-free triangular-wave topology as IFTW. Note that in the rest of this paper, we focus on the case where the data traffic is from left to right; however, the same reconfigured topology constructed from left to right will also work when the traffic direction is reversed.

### B. Channel and Antenna Models

With the standard assumption of additive white Gaussian noise channels, the link capacity is assumed to follow Shannon’s Theorem, and the rate of the directional unblocked link from node  $i$  to node  $j$  satisfies:

$$R_{i,j} \leq \beta \cdot B \cdot \log_2\left(1 + \min\left\{\frac{P_r(d)}{N_T}, T_{max}\right\}\right) \quad (2)$$

where  $B$  is channel bandwidth,  $P_r$  is the power of the intended transmitter’s signal when it reaches the receiver,  $N_T$  is the power of thermal noise,  $T_{max}$  is the upper bound of operating signal-noise ratio because of the limiting factors like linearity in the radio frequency front-end, and the link utility ratio  $\beta \in (0, 1)$ . Due to the primary interference,  $\beta \leq 0.5$  and a maximum end-to-end throughput of more than 16 Gbps can theoretically be achieved in mmWave communications [5]. Because our topology is interference-free, we can ignore the combined power of signals  $I$  from any interfering transmitters. And  $P_r$  can be calculated as follow:

$$P_r(d) = P_t \cdot G_t \cdot G_r \cdot \left(\frac{\lambda}{4\pi d}\right)^\eta \cdot e^{-\alpha d} \quad (3)$$

where  $P_t$  is the transmit power,  $G_t$  and  $G_r$  are antenna gains at transmitter and receiver, respectively,  $\lambda$  is the signal’s wavelength,  $d$  is the propagation distance,  $\eta$  is the path loss exponent, and  $\alpha$  is the attenuation factor due to atmospheric absorption. Here the small random attenuation caused by shadowing effect is ignored.

In this work, a flat-top directional antenna model is considered, i.e. transceiver antennas have a high constant gain  $G_h$  within the beam, and a very low gain  $G_l$  that can be ignored outside the narrow beamwidth  $\phi$ .

### C. Four-type Blockage Model

From Fig. 2, unlike the straight-line topology, the IFTW topology can provide alternative links through beam steering when obstacles block some of the original

links. For example,  $R_1$  can steer its TX beam to  $R_3$ 's RX beam to create an alternative link if the link from  $R_1$  to  $R_2$  (or from  $R_2$  to  $R_3$ ) is blocked. It is easy to see from Eq. 1 that these alternative links (shown with red dashed lines) will not affect the interference-free nature of the topology. Here, we describe models for the different blockage conditions that can be produced by obstacles in a roadside environment.

Based on the IFTW topology, there are some constraints for selecting alternative paths to avoid obstacles:

a) *LOS transmission constraint*: To achieve the high-throughput requirement in mmWave networks, only LOS neighbors of each node are considered as candidate nodes to be selected for next hops. For the same reason, only relatively short alternative links are considered (only the next 3 nodes are considered).

b) *TX/RX blocked constraint*: Obstacles close to a node can block multiple possible links into or out of the node. For example, an obstacle close to the transmitter side of  $N_k$  in Fig. 3 might block the main link  $P_1$  and alternative links  $P_2$  and  $P_3$ , or an obstacle very close to the receiver side of  $N_{k+1}$  could block  $P_1$ ,  $P_5$  and  $P_6$ .

c) *Primary interference constraint*: We assume that relay nodes cannot transmit and receive at the same time, which is known as the primary interference constraint. However, the secondary interference (i.e., the mutual interference resulting from concurrent transmissions on different links) can be ignored due to the narrow antenna beamwidth and with proper topology parameters.

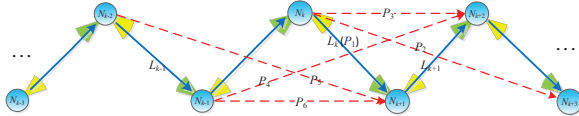


Fig. 3. Original and alternative links in the IFTW topology.

Considering these constraints, we propose a four-type blockage model. First, every obstacle that creates a blockage in the original topology must satisfy the following conditions:

- *Main link blocked condition*: At least one of the original links  $L_k$  ( $1 \leq k \leq N-1$ ) is blocked in the topology, where  $N$  is the total number of nodes.
- *Continuity of shape*: One obstacle cannot block non-adjacent links. For example, an obstacle that just blocks  $\{P_1, P_3\}$  or  $\{P_1, P_6\}$  cannot exist, but blocking  $\{P_1, P_2, P_3\}$  or  $\{P_1, P_5, P_6\}$  is possible.

**Theorem 1.** *The blockages produced by an obstacle with arbitrary shape or size can be decomposed into one or a combination of the four types in Table I.*

*Proof.* For each original main link  $L_k$  between  $N_k$  and  $N_{k+1}$  in the topology, there are 6 related paths  $P_1, \dots, P_6$  as Fig. 3 shows. And all possible paths blocked by obstacles with arbitrary shapes and locations can be summarized as following forms. For simplicity, we use “ $i_-(N_k)$ ” to indicate a *Type i* blockage for  $N_k$ , and “ $\rightarrow$ ” means the decomposed process.

1) One path blocked:  $\{P_1\} \rightarrow \{I_-(N_k/N_{k+1})\}$ .

2) Two paths blocked:  $\{P_1, P_2\} \rightarrow \{II_-(N_k)\}$ ;  $\{P_1, P_4\} \rightarrow \{III_-(N_k/N_{k+1})\}$ ;  $\{P_1, P_5\} \rightarrow \{II_-(N_{k+1})\}$ .

3) Three paths blocked:  $\{P_1, P_2, P_3\} \rightarrow \{IV_-(N_k)\}$ ;  $\{P_1, P_2, P_4\} \rightarrow \{II_-(N_k), III_-(N_k/N_{k+1})\}$ ;  $\{P_1, P_2, P_5\} \rightarrow \{II_-(N_k), II_-(N_{k+1})\}$ ;  $\{P_1, P_4, P_5\} \rightarrow \{II_-(N_{k+1}), III_-(N_k/N_{k+1})\}$ ;  $\{P_1, P_5, P_6\} \rightarrow \{IV_-(N_{k+1})\}$ .

4) Four paths blocked:  $\{P_1, P_2, P_3, P_4\} \rightarrow \{III_-(N_k/N_{k+1}), IV_-(N_k)\}$ ;  $\{P_1, P_2, P_3, P_5\} \rightarrow \{II_-(N_{k+1}), IV_-(N_k)\}$ ;  $\{P_1, P_2, P_4, P_5\} \rightarrow \{II_-(N_k), II_-(N_{k+1}), III_-(N_k/N_{k+1})\}$ ;  $\{P_1, P_2, P_5, P_6\} \rightarrow \{II_-(N_k), IV_-(N_{k+1})\}$ ;  $\{P_1, P_4, P_5, P_6\} \rightarrow \{III_-(N_k/N_{k+1}), IV_-(N_{k+1})\}$ .

5) Five paths blocked:  $\{P_1, P_2, P_3, P_4, P_5\} \rightarrow \{II_-(N_{k+1}), III_-(N_k/N_{k+1}), IV_-(N_k)\}$ ;  $\{P_1, P_2, P_4, P_5, P_6\} \rightarrow \{II_-(N_k), III_-(N_k/N_{k+1}), IV_-(N_{k+1})\}$ .

6) Six paths blocked:  $\{P_1, P_2, P_3, P_4, P_5, P_6\} \rightarrow \{III_-(N_k/N_{k+1}), IV_-(N_k), IV_-(N_{k+1})\}$ .

Thus, any blockages that take effect on different possible links can be decomposed into one or more blockages of these four types, and the proof is completed.

TABLE I  
FOUR TYPES OF BLOCKAGES AND CHARACTERISTICS

Types	Characteristics and blocked links
Type I	An obstacle in $L_k$ region just blocks the original link, such as $P_1$ in Fig. 3.
Type II	An obstacle in $L_k$ region blocks the original link and adjacent diagonal link, such as $\{P_1, P_2\}$ for $N_k$ or $\{P_1, P_5\}$ for $N_{k+1}$ .
Type III	An obstacle in $L_k$ region blocks the original link and crossed diagonal link, such as $\{P_1, P_4\}$ .
Type IV	An obstacle in $L_k$ region blocks all the TX/RX links of $N_k/N_{k+1}$ , such as $\{P_1, P_2, P_3\}/\{P_1, P_5, P_6\}$ , (equivalent to failure of node $N_k/N_{k+1}$ ).

In the face of obstacles that necessitate path reconfiguration, we consider several performance metrics. First, end-to-end throughput is critical for mmWave backhaul applications. Second, for blockage avoidance study, blockage tolerance rate (BTR) is a critical metric, which is inversely proportional to the outage probability when the end-to-end throughput is less than a threshold value, so it actually represents the high-rate connectivity tolerance in mmWave communication. Lastly, latency is also an important metric in backhaul networks.

### III. RELAY PATH SELECTION FOR OBSTACLE AVOIDANCE

In this section, we present path reconfiguration schemes for blockage avoidance in the IFTW topology. One issue to consider is whether or not the transmission schedule for nodes needs to be changed after reconfiguration. In the IFTW topology, the optimal schedule contains two transmission slots of equal length with even numbered nodes transmitting in time slot 0 and odd numbered nodes transmitting in time slot 1. This schedule achieves an optimal end-to-end throughput of  $R_{max}/2$ , where  $R_{max}$  is the data rate of each link. Allowing the transmission schedule to change provides maximum flexibility for path reconfiguration but complicates the network control protocol as new schedule information needs to be distributed to nodes after reconfiguration.

### A. Relay Path Selection with Rescheduling

In the case where an obstacle blocks one or more of the original links, let  $e_{k,k+1}$ , between node pair  $\{N_k, N_{k+1}\}$ , be the left-most blocked link in the topology. Different alternative links can be selected depending on the blockage type. In our approach,  $N_k$  and its adjacent nodes determine the blockage type, and then  $N_k$  selects an appropriate alternative link. Due to space limitations, a detailed explanation of the distributed blockage type detection (BTD) process is not presented but it can be found in a companion technical report [13]. After the BTD process, the obtained blockage type is used to help with path reconfiguration.

As mentioned earlier, only the next 3 nodes are considered as candidates for the alternate link. Thus, when one original link is blocked,  $\{L_{k-2}, L_{k-1}, L_k, S_{k-1}, S_k\}$  shown in Fig. 4 are all options for substitution. First, the BTD detection process is executed, after which node  $N_k$  and its surrounding nodes know the blockage type. Then  $N_k$  executes Algorithm 1 beginning from Line 2, as explained below. We refer to Algorithm 1 as the high-throughput path reconfiguration (HTPR) algorithm. This algorithm is repeated from left to right in the topology until no further blockages remain.

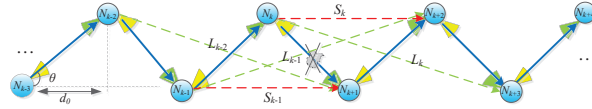


Fig. 4. Possible alternative links for blockage avoidance.

HTPR executes on a node  $N_k$  as follows. According to the blockage type, different alternative link sets  $altPath$  are obtained (Lines 2-10). The  $altPath$  set for any combination blockage case (see Theorem 1) is simply the intersection of the  $altPath$  sets of the corresponding basic types (Lines 11-12).

To achieve higher throughput, the shorter alternative links such as  $S_{k-1}$  and  $S_k$  are given priority in  $altPath$  (Lines 24-25), but if both of them are not available, other longer alternative links can be chosen. Besides, the larger-index link is preferred, e.g.  $S_k(L_k)$  has priority over  $S_{k-1}(L_{k-1})$ , because it may circumvent other obstacles that take effect on higher-numbered links (e.g. avoid the possible blockage of  $e_{k+1,k+2}$  as well). When consecutive alternative links need to be selected (e.g. if all original links are blocked), shorter and longer alternative will be assigned alternated priority to prevent the topology degenerating to a straight line, which is subject to severe self interference (Lines 26-27). Note that an alternative link can be selected (viewed as  $goodPath$ ) only if its start and end node exist in  $Path$ , and the end node is not failed (Lines 21-23).

After selecting the alternative link  $newLink$  (Lines 14-20), the no longer used nodes in  $Path$  are cleared (e.g. remove  $N_{k+1}$  from  $Path$  for selecting  $S_k$  in Fig. 4). Otherwise (i.e., no alternative paths can avoid this blockage), all nodes in  $Path$  are cleared and the process is

terminated, which means that a communication outage happens. If  $Path$  is non-empty, it is forwarded from  $N_k$  to its surrounding nodes, and each node aligns its directional TX/RX antennas based on the new path.

---

#### Algorithm 1 Finding the relay path for blockage avoidance

---

**Input:**  $Path$  (includes active nodes),  $E$  (includes each link  $e_{i,j}$ )

**Output:**  $newLink$

```

1: ( $Blink, BType$ ) =  $BTDProcessFunction(Path, E)$ 
2: switch ( $BType$ ) do
3:   case: Type I then
4:      $altPath_1 = \{S_k, S_{k-1}, L_k, L_{k-1}, L_{k-2}\}$  // in Fig. 4
5:   case: Type II for  $N_k(N_{k+1})$  then
6:      $altPath_2 = \{S_k, S_{k-1}, L_{k-1}, L_{k-2}(L_k)\}$ 
7:   case: Type III then
8:      $altPath_3 = \{S_k, S_{k-1}, L_k, L_{k-2}\}$ 
9:   case: Type IV for  $N_k(N_{k+1})$  then
10:     $altPath_4 = \{S_{k-1}(S_k), L_{k-1}, L_{k-2}(L_k)\}$ 
11:  default cases:  $combine-Type = \cup_{i \in [1,4]}(Type\ i)$  then
12:     $altPath_k = \cap_i(altPath_i)$  // intersection
13:  end switch
14:  $newLink = selectPath(altPath, Blink, Path)$ 
15: if ( $newLink \neq \emptyset$ ) then
16:    $Rmv(nodes\ btw\ newLink.src\ and\ newLink.dst\ in\ Path)$ 
17: else
18:    $Rmv(all\ nodes\ in\ Path)$  // remove all nodes
19:   break // no substituted paths, outage happens
20: end if
   Function: selectPath(altPath, Blink, Path)
21: for  $link$  in  $altPath$  do
22:    $goodPath = testIf(link.src, link.dst \in Path \ \& \ link.dst\ not\ failed)$ 
23: end for
24: if ( $N_k.preNode$  in  $Path \neq N_{k-2}$ ) then
25:    $goodPath = sortSL(goodPath)$  // shorter path first,
   then larger index first, eg. the order in  $altPath_1$ 
26: else
27:    $goodPath = sortLS(goodPath)$  // longer path first,
   then larger index first
28: end if
29: return  $newLink = goodPath(1)$ ; // get the first element

```

---

In the HTPR algorithm, because shorter alternative links are given priority, the original scheduling will be disrupted. For example,  $N_k$  and  $N_{k+2}$  were transmitting in the same time slot according to the original schedule, and if  $S_k$  is chosen,  $N_{k+2}$  cannot receive the signal from  $N_k$  due to the primary interference constraint. Thus, it is necessary to perform rescheduling after relay path selection. This becomes a general path scheduling problem, so the optimal schedule algorithm is used to perform rescheduling, where the minimum schedule length equals to the maximum time demand sum of two consecutive links in the topology [5], i.e.,

$$t_{min} = \max_{1 \leq i \leq N-1} \{T_i + T_{i+1}\} \quad (4)$$

where  $T_i$  is calculated by  $D/R_i$ ,  $D$  and  $R_i$  are the data demand and rate of each link. Thus, the rate of whole system  $R_{sys}$  is obtained by  $D/t_{min}$  in Eq. 5, which is actually determined by the bottleneck link rates.

$$R_{sys} = \left\{ \max_{1 \leq i \leq N-1} (R_i^{-1} + R_{i+1}^{-1}) \right\}^{-1} \quad (5)$$

## B. Relay Path Selection without Rescheduling

Considering the rescheduling complexity, some network scenarios might not permit modification of the transmission schedule. To handle this case, we provide two new versions of the path selection algorithm (NR-1 and NR-2) that maintain the same schedule used in the original topology. To be specific, after relay path selection by these two algorithms, each time slot length will stay the same as it was in the original IFTW topology, i.e.  $t_{slot} = D/R_{max}$  and the entire schedule length is, therefore,  $t_{min} = 2D/R_{max}$ . However, as a trade off, less data can be sent on longer alternative links that are selected for the new path, and some of the time within  $t_{slot}$  will then be unused for the shorter original links, and this leads to an overall lower system rate.

In the NR-1 algorithm, when one of the original links  $e_{k,k+1}$  is blocked, only longer alternative links can be selected for blockage avoidance, such as  $L_{k-2}$ ,  $L_{k-1}$  and  $L_k$  in Fig. 4, and only those links would be put in *altPath*. Even though these longer alternative links may become bottleneck links and degrade system throughput, they will not break the original schedule, i.e. all even-numbered and odd-numbered relay nodes from original *Path* can still transmit in their original time slots.

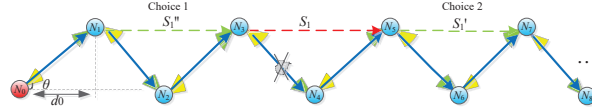


Fig. 5. Substituted relay path selection for NR-2.

The NR-2 algorithm aims to select shorter alternative links without rescheduling, which may improve the system throughput compared to NR-1. The strategy is to keep the alternative links in pairs, i.e. if one shorter alternative link is selected for blockage avoidance, it is necessary to select an adjacent shorter alternative link to keep them in pairs. In Fig. 5,  $S'_1$  and  $S''_1$  are the two possible links that can be paired with  $S_1$ . If link pair  $(S_1, S'_1)$  is chosen to avoid blockages, it is unnecessary to reschedule all nodes in the topology, but just the shared node  $N_5$  needs to switch its time slot for transmission, and all other even-numbered or odd-numbered nodes can still transmit in their original slots.

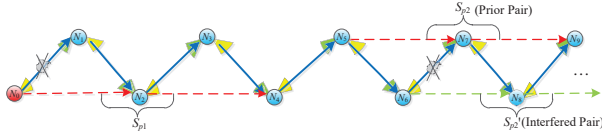


Fig. 6. Alternative selection strategy for NR-2 ( $N > 10$ ).

Particularly, for some multi-blockage cases in a long topology, the strategy is to select different-side shorter link pairs alternatively to overcome the interference effect as far as possible. As an example shows in Fig. 6, after checking the previous substituted path information from *Path* (eg.  $S_{p1}$  is on the odd-numbered node side), the leader node  $N_6$  will select the short link pairs on the even-numbered node side (such as  $S_{p2}$ ) prior to odd-numbered node side (such as  $S'_{p2}$ ), which aims

to avoid interference effects. However, when multiple blockages occur such that  $S_{p2}$  is not available, the leader node has to select  $S'_{p2}$  as substituted link. In this case, self interference along the path will occur, which will degrade system throughput.

In summary, the three path reconfiguration schemes can be used depending on the network's capabilities. HTPR algorithm can achieve high throughput and better blockage tolerance, since it considers more possible paths and shorter alternative links are usually selected. However, if the network does not support rescheduling, Algorithm NR-1 or Algorithm NR-2 can be used.

## IV. GUARANTEED RECONFIGURATION CASES

Here, we analyze the single-obstacle case under the following size constraint. Later, we also analyze the case where an arbitrary number of *Type I* blockages occur.

*Assumption 1. (Constraint of Size):* A single obstacle can block at most two consecutive original links, and its width must be less than the road width.

If vehicles are assumed to be the main obstacles occurring in practice, the size constraint is reasonable since vehicles cannot be large enough to affect links separated by hundreds of meters. The following theorem shows that both the HTPR and NR-2 algorithms can tolerate any single-obstacle scenario, unless the obstacle blocks all possible outgoing links from the source or all possible incoming links to the destination.

**Theorem 2.** *Under Assumption 1 (Constraint of Size), and assuming the source and destination nodes are not failed by a Type IV blockage, HTPR and NR-2 algorithms always find alternate paths for any single-obstacle case.*

*Proof.* Based on *Constraint of Size* in Assumption 1, a single obstacle can produce at most one *Type IV* blockage since two different-side shorter substituted paths (eg.  $S_{k-1}$ ,  $S_k$  in Fig. 4) cannot be blocked simultaneously, which means at most one relay node would be failed. Thus, in the worst case that an arbitrary obstacle makes a relay node  $N_k$  ( $1 \leq k \leq N-1$ ) failed,  $S_{k-1}$  (or  $S_{pk-1}$ ) can always be selected for blockage avoidance, and it works for each proposed relay path selection algorithm except for NR-1 since only longer alternative paths are optional. But for the failed node  $N_0$  or  $N_N$ , i.e. all TX/RX links of source/destination BS node are blocked by the *Type IV* blockage, there is no way to find a substituted link for path recovery by any algorithms, and it belongs to the inevitable blocked case, which models the real roadside scenario where a large truck parks very close to the source or destination BS.

When there is more than one obstacle in the network, it is possible that multiple original links are blocked. The following theorem shows that Algorithm HTPR can withstand an arbitrary number of *Type I* blockages. Note that this includes the case where *all* original links have *Type I* blockages.

**Theorem 3.** *If only Type I blockages occur, the HTPR algorithm always finds an alternate path.*

*Proof.* Here we consider the worst situation, i.e. *all original links blocked case*. According to HTPR algorithm, shorter or longer alternative paths (directly connect to next 2- or 3-hop node) will be selected to pass through the start node 0 to end node  $N$  in the topology. For arbitrary  $N = 2i$  or  $2i+1$  ( $i \geq 1$ ), the equation  $2m + 3n = N$  ( $m, n \geq 0, N \geq 2$ ) evidently has solutions of  $m$  and  $n$ , thus HTPR can always find  $m$  shorter-substitute paths and  $n$  longer-substitute paths to avoid blockages in every original link region. If part of original links are blocked, the same results can be easily proved in this way.

## V. NUMERICAL SIMULATIONS AND RESULTS

In this section, simulation results are provided to evaluate the proposed path reconfiguration schemes. Typical values for some fixed parameters were taken from a survey of the mmWave literature and are shown in Tab. II. We consider an IFTW topology that contains 2 BSs and 7 relay nodes to simulate an urban roadside environment. Obstacles are modeled as rectangular vehicles with random width (less than 4 m), length (less than 15 m) and center (within the road area). Obstacle orientations are the same as the road's direction.

TABLE II  
PARAMETERS OF SIMULATION ENVIRONMENT

$B$	2.16 GHz	$f_c$	60 GHz	$P_t$	10 mW
$G_{tx,rx}$	30 dBi	$\alpha$	17 dB/km	$\eta$	2.0
$\theta$	12°	$d_0$	80 m	$\phi$	15°

We first generated 300 obstacles at random and discarded the ones that had no effects on any of the original links. Doing this, we obtained an obstacle set  $BK$ , which contains around 60 obstacles of different sizes in random locations. These generated obstacles can be divided or decomposed into the four blockage types from our blockage model, and the result in Tab. III shows that the majority of blockages produced by random obstacles are *Type I* blockages.

TABLE III  
PROPORTION OF DIFFERENT BLOCKAGE TYPES IN  $BK$ .

Types	<i>Type I</i>	<i>Type II</i>	<i>Type III</i>	<i>Type IV</i>
Proportion	52.32%	15.56%	16.95%	15.17%

### A. Single-Obstacle Case

Here, we consider the different single obstacles making up the set  $BK$ . We simulated path reconfiguration using Algorithms HTPR, NR-1, and NR-2 for each of these single obstacles and the resulting average throughputs and blockage tolerance rates (BTRs) are shown in Tab. IV and compared against the throughput of the original network (no blockage (NB) case).

TABLE IV  
PERFORMANCE COMPARISON WITH NO-BLOCKAGE CASE.

Schemes/Scenario	HTPR	NR-1	NR-2	NB
Throughput(Gbps)	14.4057	11.4731	13.2353	15.8032
BTR(%)	95.24	90.48	95.24	N/A

The results show that HTPR has the best performance among the different algorithms. In particular, HTPR's

end-to-end throughput is only reduced by about 8% from the no-blockage case, while the throughput for NR-1 and NR-2 is reduced by about 27% and 16%, respectively. Both HTPR and NR-2 achieve a blockage tolerance rate of more than 95% for single obstacles, while NR-1's BTR is above 90%. Recall that the only single obstacle cases not handled by HTPR and NR-2 are if the source node or destination node of the path is completely blocked.

### B. Multiple Obstacles: Small and Large Obstacle Cases

In this part, multiple obstacles are considered and we focus on comparing the effects of small vs. large obstacles. To prevent several obstacles with the same link blocking effects, we restrict there to be at most one obstacle in each link region, so no more than 8 obstacles can occur concurrently in the network. We simulated the road scenario where obstacles (vehicles) in either small or large sizes occur in random different link regions. The widths and lengths of small-size obstacles are normally distributed as  $N(\mu=1.6, \sigma=0.5)$  and  $N(\mu=4.5, \sigma=0.8)$ . Whereas the large-size obstacles have widths and lengths with normal distributions  $N(\mu=3.0, \sigma=0.8)$  and  $N(\mu=11.0, \sigma=1.5)$ . For each of these cases and the number of obstacles ranging from 1 to 8, we performed hundreds of simulation results, which are reported in Figure 7.

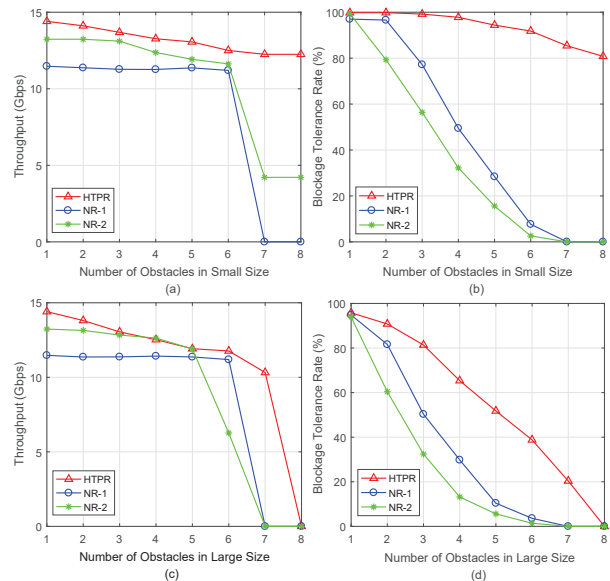


Fig. 7. Throughput/BTR vs. number of obstacles in small/large sizes.

From the results in Fig. 7(a)-(b), in addition to achieving the highest throughput, the HTPR algorithm always has the best blockage tolerance rate as the number of small obstacles increases. That is because most small-size obstacles produce *Type I* blockages, which HTPR scheme always handles (see Theorem 3). The no-reschedule algorithms, NR-1 and NR-2, have fairly good throughput performance up to about 6 obstacles but their throughputs drop dramatically for 7 or 8 obstacles. Both NR-1 and NR-2 have BTRs that decrease fairly rapidly

with the number of obstacles, and NR-1 shows better blockage tolerance than NR-2 in multi-obstacle cases.

In some extreme cases when more than 6 of the original links are blocked, the throughput of NR-2 will be lower than the minimum rate requirements for backhaul communication. These are viewed as unreconfigurable cases and, as a result, they are reported as 0% BTR. In these extreme cases, NR-2's solution degenerates to a straight-line topology, which degrades the throughput substantially due to self interference.

In Fig. 7(c)-(d), it is clear that large-size obstacles cause each algorithm to perform worse compared to the small obstacle case. This is because larger obstacles have more potential to create *Type IV* blockages, and those make a relay node failed, which leads to a decrease in the number of alternative links for path recovery. However, compared with a traditional straight-line topology, which would completely fail even with a single obstacle, each proposed algorithm based on the IFTW topology is capable of tolerating multiple failed nodes, and could still work even with up to 6 large-size obstacles in different link regions.

### C. Multiple Obstacles: Random Sizes

Now, we consider a scenario where multiple obstacles with random sizes occur in arbitrary places. Here, more than one obstacle can occur in the same link region, so several obstacles might block the same link. This models real-life scenarios where different size vehicles can be located anywhere on the road.

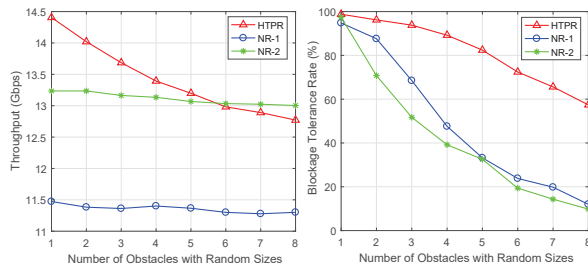


Fig. 8. Throughput and BTR comparisons vs. no. of random obstacles.

From the results in Fig. 8, we can see that all algorithms are capable of supporting end-to-end throughputs of 10+ Gbps with multiple random-sized and random-located obstacles. In terms of blockage tolerance, it is particularly notable that the HTPR algorithm has a BTR of more than 50% even with 8 obstacles impacting the 8 original links in the IFTW topology. Although HTPR's average throughput is lower than that of NR-2 for large numbers of obstacles, this is only because HTPR can reconfigure more often and the averages are computed only over the successful reconfiguration cases.

### D. Latency

To investigate how latency is impacted by path reconfiguration, we studied scenarios with several random obstacles and one packet (1KB) transmission. Since latency is impacted strongly by the number of links in the path, we also varied the number of relays. Here, the

network environment is assumed to be in good condition (no packet losses occur), hence the end-to-end latency is equal to the sum of required time slots duration.

Fig. 9 shows that latency increases only slightly (and sometimes decreases) as more obstacles occur. Thus, path reconfiguration has only a small impact on latency. The latency can decrease with more obstacles, because the reconfiguration process might drop some relay nodes, which reduces the number of required time slots for a packet to go from source to destination.

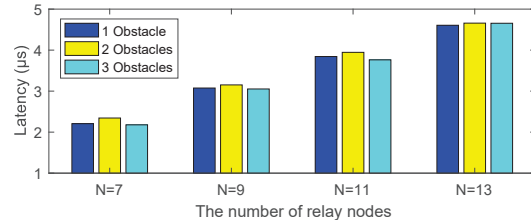


Fig. 9. Latency vs. number of obstacles and relay nodes.

## VI. CONCLUSION

In this paper, we proposed several schemes for blockage avoidance in mmWave backhaul networks based on a novel four-type blockage model in the IFTW topology. Theoretical analysis and simulation results show that the presented algorithms can support high backhaul throughputs close to the no-blockage case and are robust to multiple obstacles.

## ACKNOWLEDGEMENT

This research was supported in part by the National Science Foundation through Award CNS-1513884.

## REFERENCES

- [1] S. Rangan, et al., "Millimeter wave cellular networks: Potentials and challenge", *Proc. IEEE*, vol. 102, Mar, 2014.
- [2] Niu Y, Li Y, Jin D, et al. Blockage robust and efficient scheduling for directional mmWave WPANs[J]. *IEEE Transactions on Vehicular Technology*, 2015, 64(2): 728–742.
- [3] S. Singh, et al., "Blockage and directivity in 60 GHz wireless personal area networks: From cross-layer model to multi hop MAC design," *IEEE J. Sel. Areas Commun.*, vol. 27, no. 8, 2009.
- [4] J. Du, et al., "Gbps user rates using mmWave relayed backhaul with high gain antennas", *IEEE J. Sel. Areas Commun.*, 2017.
- [5] Qiang Hu and Douglas M. Blough, "Relay Selection and Scheduling for Millimeter Wave Backhaul in Urban Environments", *Proc. of IEEE MASS*, 2017.
- [6] Zulkuf Genc, Umar H Rizvi, Ertan Onur, et al., "Robust 60 GHz indoor connectivity: is it possible with reflections?", in *Vehicular Technology Conference (VTC 2010-Spring)*, *IEEE* 71st, 2010.
- [7] M. Park, et al., "A spatial diversity technique for IEEE 802.11ad WLAN in 60 GHz band", *IEEE Communication Letters*, 2012.
- [8] Kan Song, et al., "A fast relay selection algorithm over 60 GHz mmWave systems", *IEEE ICCT*, pp. 676–680, 2013.
- [9] X. Zhang, et al., "Improving network throughput in 60 GHz WLANs via multi-AP diversity", in *Proc. IEEE Int. Conf. Commun.*, Ottawa, ON, Canada, Jun. 10-15, 2012.
- [10] S. Biswas, S. Vuppala, J. Xue, et al., "On the performance of relay aided millimeter wave networks", *IEEE J. Sel. Topics Signal Process.*, vol. 10, no. 3, pp. 576–588, Apr. 2016.
- [11] Yong Niu, Chuhan Gao, et al., "Exploiting multi-hop relaying to overcome blockage in directional mmWave small cell", *Journal of Communications and Networks*, Vol. 18, No. 3, June. 2016.
- [12] Q. Hu and D. Blough. "Optimizing Millimeter-Wave Backhaul Networks in Roadside Environments," *Proc. of IEEE ICC*, 2018.
- [13] Yuchen Liu, Qiang Hu and Douglas M. Blough, "Technical Report for Blockage Type Detection Process". (available at: <http://blough.ece.gatech.edu/BTDTechReport.pdf>)